Title: Role of the Wilms' tumor suppressor gene *Wt1* in pancreatic development

Authors: Laura Ariza[1], Ana Cañete[1], Anabel Rojas[2], Ramón Muñoz-Chápuli[1] and Rita Carmona[1]

Email: larizamedina@hotmail.com, acansan@uma.es, anabel.rojas@cabimer.es, rita@uma.es, chapuli@uma.es

Affiliations:

[1]Department of Animal Biology, Faculty of Science, University of Málaga, 29071 Málaga (Spain) and Andalusian Center for Nanomedicine and Biotechnology (BIONAND), Malaga, Spain.

[2] Andalusian Center of Molecular Biology and Regenerative Medicine (CABIMER) and Centro de Investigación Biomédica en Red de Diabetes y Enfermedades Metabólicas Asociadas (CIBERDEM), Sevilla, Spain.

Corresponding author: Rita Carmona, Department of Animal Biology, Faculty of Science, University of Málaga, 29071 Málaga (Spain). Phone: 34-952-134135, Fax: 34-952-131668, Email: rita@uma.es

Short title: Wt1 in pancreatic development

Abbreviations

EMT: Epithelial-mesenchymal transition

GFAP: Glial fibrillary acidic protein

PSC: Pancreatic stellate cells

Abstract

The Wilms tumor suppressor gene (*Wt1*) encodes a transcription factor involved in the development of a number of organs, but the role played by *Wt1* in pancreatic development is unknown. The pancreas contains a population of pancreatic stellate cells (PSC) very important for pancreatic physiology. We described elsewhere that hepatic stellate cells originate from the WT1-expressing liver mesothelium. Thus, we checked if the developmental origin of PSCs was similar. WT1 protein is expressed in the pancreatic mesothelium. Between E10.5 and E15.5, this mesothelium gives rise to mesenchymal cells that contribute to a major part of the PSC and other cell types including endothelial cells. Most WT1systemic mutants show abnormal localization of the dorsal pancreas within the mesentery and intestinal malrotation by E14.0. Embryos with conditional deletion of WT1between E9.5 and E12.5 showed normal dorsal pancreatic bud and intestine, but the number of acini in the ventral bud was reduced about 30% by E16.5. Proliferation of acinar cells was reduced in WT1 systemic mutants, but pancreatic differentiation was not impaired. Thus, mesothelial-derived cells constitute an important subpopulation of pancreatic mesodermal cells. WT1 expression is not essential for pancreas development, although it influences intestinal rotation and correct localization of the dorsal pancreas within the mesogastrium.

Keywords: Mesothelium, epithelial-mesenchymal transition, pancreatic stellate cells, pancreatic stroma, intestinal rotation.

Introduction

The Wilms tumor suppressor gene (*Wt1*) encodes a C2H2-type zinc-finger transcription factor that can appears in mammals under different isoforms, participating in transcriptional regulation, RNA metabolism and protein-protein interactions (1-3). *Wt1* has been involved in the development of a number of organs, including kidneys and gonads (4), spleen (5), adrenals (6), liver (7,8), heart (9-11), lungs (12) and diaphragm (13). However, there are no reports in the literature about the role played by *Wt1* in pancreatic development, despite the parallelisms between liver and pancreas organogenesis.

In mouse, pancreas develops from dorsal and ventral primordia derived from the endoderm. The dorsal primordium emerges through evagination of the endodermal epithelium starting by E9.5. The ventral pancreatic bud appears later, by the stage E10.5. Splanchnic mesodermal cells induce growth and branching of these buds. The endodermal cells give rise to the main pancreatic cell types, the exocrine acinar cells, ductal cells and endocrine cells from the islets of Langerhans (14). Mesodermal cells contribute to the vascular and connective tissue of the pancreas, and also to a pancreas-specific cell type, the pancreatic stellate cells (PSCs).

In normal adult pancreas, the pancreatic stellate cells (PSCs) are quiescent, star-shaped cells with a periacinar distribution. They contain vitamin A-rich lipid droplets in the cytoplasm and exhibit positive immunostaining for desmin and glial fibrillary acidic protein (GFAP) (15). In normal pancreas, PSCs are involved in keeping the epithelial integrity of the pancreatic acini via maintenance of the basement membrane (16,17). Furthermore, when activated by profibrogenic stimuli such as inflammatory cytokines or oxidant stress, PSCs proliferate and transform into myofibroblast-like cells, becoming the major source of extracellular matrix. PSC have also recently become a focus of interest since they play a key role in pancreatic cancer, a malignancy with a high prevalence and poor prognosis (18-20). Despite this capital importance in normal and pathological conditions, the embryonic origin of PSCs remains unknown.

PSCs are similar to the hepatic stellate cells located in the perisinusoidal space of the liver. These cells share many features with PSCs and they are also involved in the fibrotic process. It has been described that the liver mesothelium contributes to the hepatic stellate cells and vascular endothelium during development (7,8). The local

emergence of mesenchymal cells through a localized epithelial-mesenchymal transition (EMT) of the coelomic epithelium or mesothelium lining developing organs has been extensively studied in some cases, such as the heart, where the epicardium gives rise to epicardial-derived cells that contribute to the cardiac vascular and connective tissues (21). In other organs, such as the lungs, liver and gut, the developmental fate of the mesothelial-derived mesenchyme and their importance for visceral morphogenesis has been also demonstrated (For a review, see ref. 22). Thus, we aimed to check if pancreatic mesothelium also supplies mesenchymal cells to the developing pancreas and if these mesenchymal cells account for the origin of PSCs.

Our results confirmed that WT1 protein is only expressed in the mesothelium of the developing pancreas, allowing for tracing of the mesothelial-derived cells with the Cre/LoxP system. During the early stages of pancreas morphogenesis, this mesothelium shows the typical features of EMT. Mesothelial-derived cells, identified by YFP expression in our model, differentiate into a major part of the PSCs and contribute to other cell types, including a part of the vascular endothelium. Conditional deletion of WT1 by the time in which the EMT process is generating the PSC, causes a delay in the growth of the ventral pancreatic bud, but the development of the dorsal bud and the PSC are normal. Systemic WT1 mutants die during the early stages of pancreatic development, but they show defects in the mesogastrium, anomalous localization of the dorsal pancreatic bud in the mesentery, intestinal malrotation and reduced proliferation of acinar cells. Thus, mesothelial-derived cells originated by an EMT constitute a significant subpopulation of mesodermal cells during pancreas development and modulate its growth, although WT1 seems to be basically dispensable for pancreatic differentiation.

Materials and methods

The animals used in our research program were handled in compliance with the institutional and European Union guidelines for animal care and welfare. The procedures used in this study were approved by the Committee on the Ethics of Animal Experiments of the University of Malaga (procedure code 2015-0028).

The Tg(Wt1-cre)#Jbeb ($Wt1^{cre}$) mouse line has been used in previous studies to trace or delete specific genes in WT1-expressing cells (11,12,23-26). For lineage tracing

studies, homozygote $Wt1^{cre+/+}$ were crossed with $Rosa26^{EYFP}$ (B6.129X1-Gt(ROSA)26Sortm1(EYFP)Cos/J) mice to generate permanent reporter expression in Wt1-expressing cells.

The Wt1tm2(cre/ERT2)Wtp/J allows for inducible Cre-recombinase expression in WT1-expressing cells after tamoxifen treatment (27). We have used this line crossed with $Rosa26^{EYFP}$ for inducible reporter expression in the WT1 lineage and also to delete expression of Wt1 in this lineage when the driver was crossed with a $Wt1^{LoxP}$ mice (10). For inducible reporter expression mice were intraperitoneally injected at different stages with tamoxifen (Sigma, T5648) dissolved in corn oil (10 mg/mL) at a dose of 0,1 mg/g body weight together with 0,05 mg/g body weight of progesterone to reduce abortion risk. In one experiment, a single dose was injected at the stage E9.5, and the embryos were fixed at E14.5. In a second experiment, three doses of tamoxifen were injected at E9.5, E10.5 and E11.5, and the embryos were fixed at E15.5 and E16.5. In the third experiment, tamoxifen was injected at E9.5, E10.5, E11.5 and E12.5 and the embryos were fixed at E16.5. We always used as controls littermates either Cre- or lacking of floxed *Wt1* alleles. No differences were observed between both types of controls. The $Wt1^{GFP}$ knockin line (28) in which the exon 1 of one Wt1 allele has been replaced by the GFP sequence, was also used as an independent reporter for active Wt1 transcription and also as a model of WT1 loss of function ($Wt1^{GFP/GFP}$).

Embryos were staged from the time point of vaginal plug observation, which was designated as the stage E0.5. Whole embryos and the viscera of neonates were excised, washed in PBS and fixed in 4 % fresh paraformaldehyde solution in PBS for 2-8 h. Then, the embryos were paraffin-embedded or washed in PBS, cryoprotected in sucrose solutions, embedded in OCT and frozen in liquid N2-cooled isopentane. Ten μm cryosections were stored at -20ºC until use.

Immunofluorescence was performed using routine protocols. Deparaffinized sections or cryosections were rehydrated in Tris-PBS (TPBS) and blocked for non-specific binding with SBT (16% sheep serum, 1% bovine albumin, 0.1% Triton X-100 in TPBS). When biotinylated secondary antibodies were used, endogenous biotin was blocked with the Avidin-Biotin blocking kit from Vector. Single immunofluorescence was performed incubating the sections with the primary antibody overnight at 4ºC, washing in TPBS and incubating with the corresponding

fluorochrome-conjugated secondary antibody. Double immunofluorescence was performed by mixing both primary antibodies (rabbit polyclonal and mouse or rat monoclonal), and incubating overnight at 4ºC. We then used a Cy5-conjugated and a biotin-conjugated secondary antibody, followed by 45 min incubation with TRITC-conjugated streptavidin. Nuclei were counterstained with DAPI (Sigma D-4592). Details of the antibodies used in this study are provided in Table 1.

For flow cytometry analysis, pancreas from $Wt1^{cre}/Rosa26R^{EYFP}$ embryos were excised, dissociated for 15 min at 37ºC in 0.1% collagenase solution in PBS and homogenized by repeated pipetting. Cell suspension was washed in PBS plus 2% fetal bovine serum and 10 mM HEPES. Then, cells were incubated on ice at the dark with Cy5-conjugated rat Anti-mouse CD31 (Pecam-1). After washing, the cells were analyzed in a MoFlo cell sorter.

For time-lapse video recording, E12.5 $Wt1^{Cre}/ROSA26R^{EYFP}$ mouse embryos were dissected in sterile PBS. Caudal stomach and proximal duodenum were isolated and cultured as previously described (29). Basically, organ explants were transferred to coverglass bottomed dishes coated with 20 µl Matrigel™ and placed in a 37°C incubator for 20 min to solidify the Matrigel™. The rudiments were then covered with medium (DME H-16/F-12 1:1 supplemented with 10% FBS, antibiotics and insulin-transferrin-selenium). After 24 h of culture, images were captured in a Leica SP5 confocal microscope every 5 min for 6 h. During the capture, the culture chamber was maintained at 37°C in a 5% CO_2 humidified atmosphere.

Analysis of the differences between dorsal and ventral pancreatic buds was performed on images taken from paraffin sections of four E16.5 $Wt1^{creERT2};Wt1^{flox}$ mutants and four control littermates, using between 4-6 images for each embryo. In total, 39 sections were analysed. The contour of the dorsal and ventral pancreatic buds were drawn, and the acini were manually recorded for each section. Number of acini and surface of the pancreatic contours were calculated using ImageJ software. The mean values obtained for each embryo were compared using Student's t-test, since the KS test found the data consistent with a normal distribution.

For the proliferation study, the acinar surface was measured as described above and the number of $PH3^+$ acinar cells counted (N=6 systemic mutants and 8 controls, 15

and 20 sections analysed, respectively). Since one of the data sets was not consistent with a normal distribution, U-Mann Whitney test was used to compare the values obtained.

Results

Pancreatic mesothelium expresses WT1 and gives rise to mesenchymal cells during development

WT1 expression in the pancreas is basically restricted to the mesothelium in all the stages studied. A faint WT1 immunoreactivity can be seen in a few submesothelial cells from early (E12.5-E13.5) embryos suggesting downregulation of WT1 expression during the EMT of the mesothelium, as described in other organs (12). However, no WT1 expression was detected in the mesoderm surrounding the pancreatic epithelium (Figure 1A-C). Thus, the driver $Wt1^{Cre}$ is a reliable marker for the mesothelial-derived cells during pancreatic development.

Morphological features of EMT were observed in the pancreatic mesothelium at the earliest stages studied (E12.5 and E13.5), including discontinuous laminin immunoreactivity, reduced E-cadherin expression, loose lateral adhesion between mesothelial cells and basal cytoplasmic processes (Figure 1D-F). These signs coincided with a punctate pattern of cytokeratin immunostaining in the submesothelial cells, suggesting collapse of the epithelial-type cytoskeleton (Figure 1E). Continuous laminin immunoreactivity appears in the basal lamina of the pancreatic mesothelium by E15.5, and mesothelial cells express E-cadherin in later stages (Figure 1G,H), suggesting a downregulation of the EMT process. RALDH2, the main enzyme for retinoic acid synthesis in the mesoderm, was immunolocalized in the pancreatic mesothelium at all the stages studied (Figure 1H).

Time lapse video recording of pancreatic explants obtained from E12.5 $Wt1^{cre}$;$R26R^{EYPF}$ embryos showed areas of EMT where YFP^+ cells were migrating from the mesothelium towards the growing acini (Supplemental Figure 1A,C and Supplemental video 2). However other areas showed a thick, quiescent mesothelium lacking of signs of EMT (Supplemental Figure 1B and Supplemental video 1). Interestingly, YFP^+ cells were observed migrating and intercalating between the branching acini (Supplemental Figure 1D and Supplemental video 3).

Cell counts on confocal images taken from two E12.5 $Wt1^{cre}$;$R26R^{EYPF}$ embryos (four images each) show that 58.6±2.1% of the mesenchymal cells of the pancreas are YFP^+, and thus they belong to the WT1-expressing cell lineage. Induction of the Cre-recombinase expression by E9.5 in the $Wt1^{creERT2}$;$R26R^{EYFP}$ model provoked the staining of very few cells in the pancreatic stroma of E14.5 embryos (Figure 1I), contrasting with the massive staining of Sertoli cells in the testis. However, induction between E9.5 and E11.5 greatly increased the number of stromal YFP^+ cells by E15.5 (Figure 1J). This suggests that most cells derived from the WT1-expressing cell lineage (i.e. putative mesothelial-derived cells) originate after E10.5, when the pancreatic buds start growing.

A major part of pancreatic stellate cells derives from the WT1-expressing cell lineage

YFP colocalized with desmin, a marker of PSC, in many periacinar mesenchymal cells from the $Wt1^{cre}$;$R26R^{EYPF}$ embryos from E14.5 on (Figure 2A,B). Some of these cells project thin cytoplasmic projections between the acinar cells, a characteristic feature of PSC (Figure 2A). WT1-expressing lineage cells also contribute to the subpopulation of desmin-positive, islet PSC (Figure 2B). Colocalization of YFP with GFAP, another marker of pancreatic stellate cells, confirmed the mesothelial origin of islet PSC in older embryos, about E18.5 (Figure 2C). No differences were found between dorsal and ventral pancreatic buds in the contribution of WT1-expressing lineage cells (Supplemental Figure 2)

The contribution from mesothelial-derived cells to the vascularization of the pancreas was also studied. A number of perivascular cells expressing NG2 (a pericyte marker) are YFP^+ (Figure 2D), and YFP also colocalized with the endothelial marker CD31/Pecam-1 (Figure 2E,F).

In order to confirm and to quantify the contribution of YFP^+ cells to the pancreatic endothelium we performed analytic flow cytometry of disaggregated pancreas obtained from four E14.5 embryos. The results (Figure 3) show that about a third of all the pancreatic cells by this stage belongs to the WT1-expressing cell lineage (34,7%±1,9, mean±SEM, n=4). 3,1%±0,2 of the total cells analysed are endothelial and from them, 9,2%±1,1 are YFP+.

Wt1 deletion in mesothelium causes a delay in ventral pancreas growth, defective mesogastrium, abnormal dorsal pancreas location and intestinal malrotation

In order to check if WT1 expression is required for pancreatic development we studied both, embryos with systemic deletion of WT1 ($Wt1^{GFP/GFP}$) and $Wt1^{creERT2}$;$Wt1^{flox}$ embryos induced with tamoxifen at different times. Most systemic WT1-null embryos die before the stage E13.5 and their pancreas are too small in order to detect anomalies in their development. The eight $Wt1^{GFP/GFP}$ embryos obtained by the stages E13.5 and 14.5 showed pancreas of similar size when compared with the control heterozygote littermates ($Wt1^{GFP/+}$) (Figure 4A-H). However, these embryos with loss of WT1 function showed defective development of the mesogastrium, leading to an abnormal location of the dorsal pancreas, that was embedded in the mesenteric wall. In one case, pancreatic tissue was observed inside the liver, due to this anomalous position (Figure 4G). Surprisingly, in six out the eight mutant embryos analysed the duodenum was located close to the larger curvature of the stomach, at the left side, suggesting an intestinal malrotation (Figure 4E-H). In some of these cases the hindgut was abnormally placed at the right side (Figure 4E,F).

Tamoxifen treatment of $Wt1^{creERT2}$;$Wt1^{flox}$ embryos between E9.5 and E11.5 (three doses) and fixed at stages E15.5 and E16,5 suppressed WT1 expression in the pancreas (Figure 4I,J), but this deletion did not cause differences in pancreatic development (not shown). However, WT1 deletion induced between E9.5 and E12.5 (four doses) and analysed at E16.5 showed a significant delay in the development of the ventral pancreatic bud, characterized by a smaller number and smaller density of acini as compared with the controls (Figures 4K,L and 5A,B). However, anomalies were not found in dorsal pancreatic buds, intestine or mesogastrium in these mutant embryos. (Figure 4K,L).

We then studied the proliferation of the pancreatic acinar cells in systemic $Wt1^{GFP/GFP}$ mutant embryos by immunolocalization of phosphohistone-H3 (Figure 5C). The mitotic rate (expressed as number of PH3+ cells by acinar surface) was significantly lower than the obtained from control $Wt1^{GFP/+}$ littermates when we considered dorsal and ventral pancreas together ($p=0.012$, U Mann-Whitney test, Figure 5C). Dorsal and ventral mutant pancreas considered separately showed a trend to reduced proliferation, very close to statistical significance ($p=0.06$ and $p=0.08$, respectively).

All E16.5 control and mutant embryos with conditional deletion of Wt1 showed similar immunoreactive patterns of amylase, insulin, glucagon, Ptf1a, mucin, desmin, E-cadherin, PDX1, neurogenin and RALDH2 (some examples shown in Suppl. Figure 3). This suggests that the developmental delay did not affect the pancreatic differentiation. Particularly, the number of desmin+, pancreatic stellate cells was similar in both, conditional *Wt1* mutant and control embryos.

Adult mesothelium does not contribute to renewal of the pancreatic stellate cell population

In order to check if the adult mesothelium is still contributing to the stellate cell population in adult mice we induced *Wt1* reporter expression in a $Wt1^{cre}$;$R26R^{EYPF}$ adult mouse (four weeks old) and then we checked the presence of YFP+ stellate cells in the pancreas after one month. The pancreatic mesothelium was YFP+, but no positive cells were found inside the pancreas, thus suggesting the lack of a postnatal contribution of the mesothelium to the pancreatic stellate cells (Suppl. Figure 4).

Discussion

We show in this paper that the pancreas, as described for other viscera (for a review, see ref. 22), receives a substantial contribution of mesothelial-derived cells originated by a process of epithelial-mesenchymal transition. Our findings confirm, using a genetic model of lineage tracing, the recently published results obtained by direct labeling of the pancreatic mesothelium (30). We have also shown that WT1 is expressed in the embryonic mesothelium of the pancreas and it is rapidly downregulated as mesenchymal cells arise from it and migrate into the developing organ, intercalating between the branching endodermal tissue. Thus, $Wt1^{Cre}$ is a reliable driver for cell tracing of the mesothelial-derived cells during pancreatic development. The main part of this process of generation of pancreatic stroma occurs between E10.5 and E14.5, as suggested by the scarce labelling of mesenchymal cells when reporter activation is performed by E9.5 and by the epithelialization of the pancreatic mesothelium and the disappearance of EMT signs by E15.5. Mesothelial-derived cells contribute to the vascularization of the developing pancreas giving rise to a minor part of the endothelium (about 10% by midgestation) and perivascular cells. Furthermore, as it has been also described for other developing organs, mesothelial-derived cells contribute to an organ-specific cell type, the pancreatic stellate cells, including the subtype known as

islet stellate cells (31). This contribution is significant, accounting for more than a half of the PSC by midgestation. In adults, we have seen that about 15-30% of the PSC still belong to a WT1-expressing lineage (not shown), but a postnatal contribution of the mesothelium to the PSC population seems not significant (Suppl. Figure 4). However, we cannot conclude that the adult PSC of the WT1-expressing lineage have originated from the embryonic mesothelium, since postnatal expression of WT1 occurs during PSC activation (ref. 32 and our unpublished observations). Anyhow, the embryonic origin of the PSC shows commonalities with the origin of the similar hepatic stellate cells, many of them also emerging from the embryonic mesothelium (7,8).

Despite this significant contribution of WT1-expressing cells to the pancreatic stroma, WT1 seems to be basically dispensable for pancreas development, differently to many other viscera, as detailed in the introduction. After conditional WT1 deletion between E9.5 and E12.5, pancreatic bud develops normally at least until E16.5, although the growth of the ventral pancreatic bud growth is delayed, showing a 30% reduction in the number and density of acini. This delay can be explained by the decrease in proliferation of endodermal cells that we have observed in systemic WT1 mutants between E13.5 and E14.5. The reduced proliferation suggests some kind of WT1-dependent signaling mechanism acting in the mesothelial-derived cells. In fact, the liver size is also hypoplasic in WT1-null mice (7).

Pancreatic size was normal in E13.5 and E14.5 WT1 systemic mutants (the oldest stage reached by these embryos). However, the mesogastrium showed defective development and, as a consequence, the dorsal pancreatic bud was mislocated into the dorsal mesentery. Unexpectedly, in six out eight WT1 systemic mutants we observed an intestinal malrotation, with the duodenum placed at the left side, along the greater curvature of the stomach. This phenotype does not appear in the conditional WT1 deletion performed between E9.5 and E12.5. Thus, early WT1 expression (before E9.5) seems to be required for the development of the mesogastrium and the correct rotation of the intestine. A similar phenotype of intestinal malrotation has been described in mice with loss of function of both, the homeodomain transcription factors BARX1 and PITX2 (33,34). Importantly, BARX1 loss of function leads to decreased expression of WT1 (35). Thus, WT1 is involved in L-R patterning of the intestine, probably through its role in the development of the mesogastrium and mesenteries. In fact, WT1 function

is critical for the organization of other coelomic components, such as the pleuropericardial membranes (9) and the diaphragm (13).

We could not study further pancreatic development in older systemic WT1 mutant embryos due to the mortality caused by defects in other viscera (basically the heart). Thus, we cannot know if the difference between dorsal and ventral buds can expand in later stages, or if the formation of the endocrine pancreas might be compromised by the lack of WT1.

In summary, the pancreas becomes a new addition to the list of organs whose morphogenesis is regulated by WT1, although in this case the impact of the WT1 loss of function is very low as compared with other viscera as the heart, kidney, adrenals, gonads or spleen, i.e. the mesodermal organs. The situation is similar to that described in other endodermal organ, the liver, where the lack of WT1 only results in a reduced size and an abnormal lobing (7). The pancreatic stroma, as described for many other viscera, shows also a mixed origin, from the splanchnopleural mesoderm and from WT1-expressing mesothelial-derived cells. Finally, we have shown that an organ-specific cell type, the PSC, can also originate from embryonic mesothelium, as occurs in the testicle (Sertoli cells), ovary (granulosa cells) or intestine (Cajal interstitial cells) (for a review, see ref. 22).

Author Contributions

R. Carmona, L. Ariza and R. Muñoz-Chápuli designed research, analyzed data and wrote the paper. R.Carmona, L. Ariza, A. Cañete and A. Rojas performed research.

Acknowledgments

We thank Dr. John Burch (National Institutes of Health) for the gift of the Wt1-Cre mice, and David Navas (SCAI, University of Málaga) for technical help with confocal microscopy and flow cytometry. This work was supported by the Spanish Ministry of Economy and Competitiveness under Grant BFU2014-52299-P; Instituto de Salud Carlos III-TERCEL network under Grant RD12/0019-0022; and Junta de Andalucía under Grant P11-CTS-07564.

References

1. Morrison, A.A., Viney, R.L., and Ladomery, M.R. (2008) The post-transcriptional roles of WT1, a multifunctional zinc-finger protein. *Biochim. Biophys. Acta* **1785**,55-62

2. Hohenstein, P., and Hastie, N.D. (2006) The many facets of the Wilms' tumour gene, WT1. *Hum. Mol. Genet*. 15 Spec No 2:R196-201

3. Toska, E., and Roberts, S.G. (2014) Mechanisms of transcriptional regulation by WT1 (Wilms' tumour 1). *Biochem. J.* **461,**15-32

4. Kreidberg, J.A., Sariola, H., Loring, J.M., Maeda, M., Pelletier, J., Housman, D., and Jaenisch, R. (1993) WT-1 is required for early kidney development. *Cell* **74**,679-691

5. Herzer, U., Crocoll, A., Barton, D., Howells, N., and Englert, C. (1999) The Wilms tumor suppressor gene Wt1 is required for development of the spleen. *Curr. Biol.* **9**,837–840

6. Moore, A.W., McInnes, L., Kreidberg, J., Hastie, N.D., Schedl, A. (1999) YAC complementation shows a requirement for Wt1 in the development of epicardium, adrenal gland and throughout nephrogenesis. *Development* **126,**1845-57

7. IJpenberg, A., Pérez-Pomares, J.M., Guadix, J.A., Carmona, R., Portillo-Sánchez, V., Macías, D., Hohenstein, P., Miles, C.M., Hastie, N.D., and Muñoz-Chápuli R. (2007) Wt1 and retinoic acid signaling are essential for stellate cell development and liver morphogenesis. *Dev. Biol.* **312,**157-70

8. Asahina, K., Zhou, B., Pu, W.T., and Tsukamoto, H. (2011) Septum transversum-derived mesothelium gives rise to hepatic stellate cells and perivascular mesenchymal cells in developing mouse liver. *Hepatology* **53,** 983-95

9. Norden, J., Grieskamp, T., Lausch, E., van Wijk, B., van den Hoff, M.J., Englert, C., Petry, M., Mommersteeg, M.T., Christoffels, V.M., Niederreither, K., and Kispert, A. (2010) Wt1 and retinoic acid signaling in the subcoelomic mesenchyme control the development of the pleuropericardial membranes and the sinus horns. *Circ. Res.* **106,** 1212-20

10. Martínez-Estrada, O.M., Lettice, L.A., Essafi, A., Guadix, J.A., Slight, J., Velecela, V., Hall, E., Reichmann, J., Devenney, P.S., Hohenstein P., Hosen, N., Hill, R.E., Muñoz-Chapuli, R., and Hastie, N.D. (2010) Wt1 is required for cardiovascular progenitor cell formation through transcriptional control of Snail and E-cadherin. *Nat. Genet.* **42**,89-93

11. Cano, E., Carmona, R., Ruiz-Villalba, A., Rojas, A., Chau, Y.Y., Wagner, K.D., Wagner, N., Hastie, N.D., Muñoz-Chápuli, R., and Pérez-Pomares, J.M. (2016) Extracardiac septum transversum/proepicardial endothelial cells pattern embryonic coronary arterio-venous connections. *Proc. Natl. Acad. Sci. U S A* **113,** 656-61

12. Cano, E., Carmona, R., and Muñoz-Chápuli, R. (2013) Wt1-expressing progenitors contribute to multiple tissues in the developing lung. *Am. J. Physiol. Lung Cell Mol. Physiol*. **305,** 322–332

13. Carmona, R., Cañete, A., Cano, E., Ariza, L., Rojas, A., and Muñoz-Chápuli, R. (2016) Conditional deletion of WT1 in the septum transversum mesenchyme causes congenital diaphragmatic hernia in mice. *Elife* 5. pii: e16009

14. Kim, S.K., and Hebrok, M. (2001) Intercellular signals regulating pancreas development and function. *Genes Dev.***15,** 111-27

15. Omary, M.B., Lugea, A., Lowe, A.W., and Pandol, S.J. (2007) The pancreatic stellate cell: a star on the rise in pancreatic diseases. *J. Clin. Invest.* **117,** 50-9

16. Riopel, M.M., Li, J., Liu, S., Leask, A., and Wang, R. (2013) β1 integrin-extracellular matrix interactions are essential for maintaining exocrine pancreas architecture and function. *Lab. Invest.* **93,** 31-40

17. Means, A.L. (2013) Pancreatic stellate cells: small cells with a big role in tissue homeostasis. *Lab. Invest.* **93,** 4-7

18. Chronopoulos, A., Robinson, B., Sarper, M., Cortes, E., Auernheimer, V., Lachowski, D., Attwood, S., García, R., Ghassemi, S., Fabry, B., and Del Río Hernández, A. (2016) ATRA mechanically reprograms pancreatic stellate cells to suppress matrix remodelling and inhibit cancer cell invasion. *Nat. Commun.***7,** 12630

19. Karnevi, E., Rosendahl, A.H., Hilmersson, K.S., Saleem, M.A., and Andersson, R. (2016) Impact by pancreatic stellate cells on epithelial-mesenchymal transition and pancreatic cancer cell invasion: Adding a third dimension in vitro. *Exp. Cell Res.* **346,** 206-15

20. Pothula, S.P., Xu, Z., Goldstein, D., Pirola, R.C, Wilson, J.S., and Apte, M.V. (2016) Key role of pancreatic stellate cells in pancreatic cancer. *Cancer Lett.* **381,** 194-200

21. Ruiz-Villalba, A., and Pérez-Pomares, J.M. (2012) The expanding role of the epicardium and epicardial-derived cells in cardiac development and disease. *Curr Opin Pediatr.* **24,** 569-76

22. Ariza, L., Carmona, R., Cañete, A., Cano, E., and Muñoz-Chápuli, R. (2016) Coelomic epithelium-derived cells in visceral morphogenesis. *Dev. Dyn.* **245,** 307-22

23. Del Monte, G., Casanova, J.C., Guadix, J.A,, MacGrogan, D., Burch, J.B., Pérez-Pomares, J.M., and de la Pompa, J.L. (2011) Differential Notch signaling in the epicardium is required for cardiac inflow development and coronary vessel morphogenesis. *Circ. Res.* **108,** 824–836

24. Wessels, A., van den Hoff, M.J., Adamo, R.F., Phelps, A.L., Lockhart, M.M., Sauls, K., Briggs, L.E., Norris, R.A., van Wijk, B., Pérez-Pomares, J.M., Dettman, R.W., and Burch, J.B. (2012) Epicardially derived fibroblasts preferentially contribute to the parietal leaflets of the atrioventricular valves in the murine heart. *Dev. Biol.* **366,** 111–124

25. Carmona, R., Cano, E., Mattiotti, A., Gaztambide, J., and Muñoz-Chápuli, R. (2013) Cells derived from the coelomic epithelium contribute to multiple gastrointestinal tissues in mouse embryos. *PloS One* 8:e55890

26. Casanova, J.C., Travisano, S., and de la Pompa, J.L. (2013) Epithelial-to-mesenchymal transition in epicardium is independent of Snail1. *Genesis* **51,** 32-40

27. Chau, Y.Y., Brownstein, D., Mjoseng, H., Lee, W.C., Buza-Vidas, N., Nerlov, C., Jacobsen, S.E., Perry, P., Berry, R., Thornburn, A., Sexton, D., Morton, N., Hohenstein, P., Freyer, E., Samuel, K., van't Hof, R., and Hastie, N. D. (2011) Acute multiple organ failure in adult mice deleted for the developmental regulator Wt1. *PLoS Genet.* 7:e1002404

28. Hosen, N., Shirakata, T,. Nishida, S., Yanagihara, M., Tsuboi, A., Kawakami, M., Oji, Y., Oka, Y., Okabe, M., Tan, B., Sugiyama, H., Weissman, I.L. (2007) The Wilms' tumor gene WT1-GFP knock-in mouse reveals the dynamic regulation of WT1 expression in normal and leukemic hematopoiesis. *Leukemia* **21**:1783-1791

29. Puri, S., Hebrok, M. (2007) Dynamics of embryonic pancreas development using real-time imaging. *Dev. Biol.* **306**, 82-93

30. Angelo, J.R., Tremblay, K.D. (2018) Identification and fate mapping of the pancreatic mesenchyme. *Dev. Biol.* **435**, 15-25

31. Zha, M., Li, F., Xu, W., Chen, B., and Sun, Z. (2014) Isolation and characterization of islet stellate cells in rat. *Islets* 6(2):e28701

32. Regel, I., Dreyer, T., Wuschek, A., Hausmann, S., Benitz, S., Schäffer, I., Raulefs, S., Kong, B., Steiger, K., Esposito, I., Erkan, M., Kleeff, J., and Michalski, C.M. (2015) Mesenchymal Wt1 positive stellate cells represent a minor source of the fibrotic response in pancreatitis. *Pancreatology* **15,** S2

33. Jayewickreme, C.D., Shivdasani, R.A. (2015) Control of stomach smooth muscle development and intestinal rotation by transcription factor BARX1. *Dev. Biol.* **405**, 21-32

34. Shiratori, H., Yashiro, K., Shen, M.M., Hamada, H. (2006) Conserved regulation and role of Pitx2 in situs-specific morphogenesis of visceral organs. *Development* **133**, 3015-3025

35. Kim, B.M., Miletich, I., Mao, J., McMahon, A.P., Sharpe, P.A., Shivdasani, R.A. (2007) Independent functions and mechanisms for homeobox gene Barx1 in patterning mouse stomach and spleen. *Development* **134**, 3603-3613

Figure Legends

Figure 1. Origin of pancreatic stromal cells from the embryonic mesothelium. **A-C.** $Wt1^{Cre}$;$R26R^{EYFP}$ embryo, E12.5 (A), E13.5 (B) and E15.5 (C). Wt1 protein is shown in red and the YFP reporter of the Wt1 lineage is shown in green. Actual Wt1 expression is restricted to the pancreatic mesothelium in all cases (arrows), although cells of the Wt1 lineage are already present in the pancreatic stroma by E12.5, where a faint Wt1 immunoreactivity can be seen in a few submesothelial cells (arrowheads in A). **D.** $Wt1^{Cre}$;$R26R^{EYFP}$ embryo, E12.5. Laminin immunoreactivity is shown in red. The basal lamina is disorganized in areas where YFP+ cells are more abundant (insert) suggesting epithelial-mesenchymal transition. **E.** $Wt1^{Cre}$;$R26R^{EYFP}$ embryo, E12.5. Cytokeratin immunoreactivity (in red) shows a characteristic punctiform pattern in mesenchymal cells, suggesting collapse of the cytokeratin cytoskeleton, another feature of epithelial-mesenchymal transition (insert). **F.** $Wt1^{Cre}$;$R26R^{EYFP}$ embryo, E12.5. E-cadherin immunoreactivity (red) is lacking in areas of the mesothelium by this stage (upper insert) while other mesothelial cells show E-cadherin immunoreactivity (lower insert). Loss of E-cadherin expression in an epithelium is another feature of epithelial-mesenchymal transition. **G.** $Wt1^{Cre}$;$R26R^{EYFP}$ embryo, E15.5. Laminin (red) is detected by this stage in a continuous basal lamina of the mesothelium (arrows). **H.** Immunolocalization of E-Cadherin (red) and RALDH2 (green) in an E15.5 embryo. Epithelialization of the mesothelium at this stage is demonstrated by expression of E-cadherin between mesothelial cells (arrows). **I.** $Wt1^{CreERT2}$;$R26R^{EYFP}$ embryo, E14.5. Expression of the reporter YFP (green) was induced at E9.5. Only a few cells appear labelled in the pancreatic stroma, suggesting a later origin for the mesothelial-derived cells. However, positive cells are very abundant in the Sertoli cells of the testis (T). **J.** $Wt1^{CreERT2}$;$R26R^{EYFP}$ embryo, E15.5, with reporter induction between the stages E9.5 and E11.5. Mesothelial-derived cells, belonging to the Wt1-expressing lineage, are far more abundant than in the previous case. I: intestine; LI: liver; P: pancreas; ST: stomach. Scale bars=50 μm, except A,H (25 μm) and I (100 μm).

Figure 2. Developmental fate of the Wt1-expressing cell lineage in $Wt1^{Cre}$;$R26R^{EYFP}$ embryos. **A-B.** Desmin, a marker of pancreatic stellate cells (PSC), colocalizes with YFP (arrows) in many cells of the developing pancreas by the stages E15.5 (A) and E18.5 (B). The thin prolongations of PSC can be seen between acinar cells (arrowheads in A). In the E18.5 embryo YFP+/Desmin+ cells can be seen in a developing islet (IS)

(arrowhead in B). These probably are islet stellate cells. Note colocalization around a vessel (V). The musculature of the intestine (I) is also desmin immunoreactive. **C.** Glial-fibrillary acid protein (GFAP) also colocalizes with YFP in some presumptive islet pancreatic stellate cells by the stage E18.5 (arrows). GFAP+ nerve fibers (NF) can be seen around a vessel. **D.** Neuron glia antigen-2 (NG2), a marker of pericytes and other perivascular cells colocalizes with YFP in the wall of the developing pancreatic vessels and capillaries (arrows) (stage E18.5). **E-F.** Colocalization of Pecam-1/CD31 with YFP in the pancreatic endothelium (arrows) by E16.5 (E) and E18.5 (F). Note the presence of YFP+ cells in the media of the developing arteries (arrowheads). Scale bars=50 μm.

Figure 3. Analytical cytometry of developing pancreas at the stage E14.5. Representative experiment of the data obtained from four embryos. About 10% of all the endothelial cells are YFP+ (i.e., derived from a Wt1-expressing cell lineage). About 35% of the pancreatic cells, by this stage, are derived from the same lineage.

Figure 4. Pancreatic phenotype after systemic ($Wt1^{GFP/GFP}$) and conditional (Wt1 $Wt1^{creERT2}$;$Wt1^{flox}$) embryos. **A-H.** E13.5-E14-5 embryos with systemic deletion of Wt1 (B,D-H) and control littermate (A,C). The dorsal mesogastrium (MG) is thickened in the mutant shown in B and D and remains largely attached to the mesentery (ME). The dorsal pancreatic bud is covered by the mesothelium (M) in the control, but this occurs only partially in this mutant, that shows the pancreas partially located in the mesentery (ME)(C,D). Note the abnormal development of the mesonephros (MN, arrows in B), gonads (G) and adrenals (AD) in the mutant embryo, as well as the hypoplastic liver (L). In the mutant embryos shown in panels E-H, the phenotype is more severe, the ventral mesogastrium is absent and the dorsal pancreas is embedded in the mesentery. In one case, the dorsal pancreas grows into the liver (panel G). In these mutant embryos the intestine is abnormally rotated, and the duodenum (D) is located at the left side, close to the stomach (ST). In two mutant embryos the hindgut (HG) is also malpositioned at the left side (panels G,H) PV: ventral pancreatic bud.. **I,J.** Wt1 is efficiently deleted in the mesothelium of the ventral bud of the pancreas of E15.5 $Wt1^{creERT2}$;$Wt1^{flox}$ embryos after tamoxifen treatment between E9.5 and E11.5. **K,L.** Deletion of Wt1 by tamoxifen treatment between E9.5 and E12.5 causes a delay in the development of the ventral pancreatic bud, whose acini appear more disperse in this E16.5 embryo. No differences can be found in the dorsal pancreatic bud, mesogastrium

or duodenum. Note the lack of kidneys (K) and the normal mesogastrium in the mutant embryo. Scale bars=500 μm, except C,D (100 μm) and I,J (50 μm)

Figure 5. A,B. Results of image analysis on histological sections from E16.5 $Wt1^{creERT2}$;$Wt1^{flox}$ and control embryos, treated with tamoxifen between E9.5 and E12.5. **A**: Average number of acini in the dorsal (D) and ventral (V) pancreatic buds from four conditional mutant and four control embryos. Between 4 and 6 sections were analyzed from each embryo (39 sections in total). **B**: Acinar density calculated by number of acini/pancreatic surface. Both, number and density of acini in the mutant ventral bud were significantly lower as compared with the controls (* = $p<0.05$; ** = $p<0.01$). No differences were found between the dorsal pancreatic buds. **C:** Box plots of the frequency of PH3+ cells by acinar surface in dorsal and ventral pancreas of E13.5-E14.5 WT1 systemic mutants. The horizontal bar represents the median, the boxes contain the values between the Q1 and Q3 quartiles and the vertical bars represent the full range of the values. A significant reduction ($p<0.05$, U Mann-Whitney test) was found when the data from dorsal and ventral pancreas were gathered and compared with the controls (N=6 mutants, 8 controls). Proliferation index was also lower in dorsal and ventral pancreas separately, but the differences were not significant at the $p<0.05$ level ($p=0.06$ and 0.08, respectively).

Supplemental Figure 1. Frames obtained from time lapse videos of a $Wt1^{Cre}$;$R26R^{EYPF}$ cultured pancreatic explant. **A.** Clear field image of the explant, marking the areas where the frames shown in panels B, C and D were obtained. **B.** Area of quiescent mesothelium, which appears thick and lacks of signs of epithelial-mesenchymal transition (EMT). **C.** Area of active mesothelium, showing signs of EMT. The cells marked with coloured dots are migrating towards the acini located at the right of the figure. **D.** Group of developing acini. YFP+ cells can be seen intercalating between the branching endodermal tissue (arrows).

Supplemental Figure 2. $Wt1^{Cre}$;$R26R^{EYPF}$ E16.5 embryo. No differences were found in the contribution of YFP+ cells in the dorsal and ventral pancreas. In both cases we can see contribution to desmin-expressing and endomucin-expressing cells (arrows).

Supplemental Figure 3. Histological sections from E16.5 $Wt1^{creERT2}$;$Wt1^{flox}$ and control embryos, treated with tamoxifen between E9.5 and E12.5. Despite the conditional deletion of Wt1, the differentiation of the pancreas appears normal as suggested by the expression of mucin, amylase, insulin, desmin or RALDH2.

Supplemental Figure 4. Induction of Wt1 reporter expression in a $Wt1^{Cre}$;$R26R^{EYPF}$ adult mouse (four weeks old). After one month, the pancreatic mesothelium was YFP+, but no positive cells were found inside the pancreas, suggesting lack of postnatal contribution of mesothelial-derived cells to this organ.

Supplemental videos. Time-lapse video recording of cultured pancreatic explants from E12.5 Wt1cre/ROSA26R-EYFP mouse embryos. The videos were obtained after 24 h of culture. The frames shown in supplemental figure 1 were obtained from these videos. Video 1: Area of quiescent mesothelium; Video 2: Area of activated mesothelium, showing signs of epithelial-mesenchymal transition; Video 3: group of developing acini (dark circular areas). YFP+ cells can be seen intercalating between the acini.

Table 1. Antibodies used in this study

Antibody	Supplier	Clone or Ref.	Dilution
Monoclonal rat Anti-mouse CD31 (PECAM)	Pharmingen	Ref. 550274	1/20
Monoclonal mouse anti alpha smooth muscle actin	Sigma	Clone 1A4 Ref. A2547	1/100
Rabbit polyclonal anti-pan cytokeratin	Dako	Ref. Z0622	1/100
Rabbit polyclonal anti-laminin	Sigma	Ref. L9393	1/200
Rabbit polyclonal anti-alpha NG2	Abcam	Ref. ab 5320	1/50
Rabbit polyclonal anti-ALDH1A2	Abcam	Ref. ab75674	1/200
Rabbit polyclonal anti-phosphohistone H3	Millipore	Ref. 06-570	1/100
Chicken polyclonal anti-GFP	Abcam	Ref. ab 13970	1/200
Mouse monoclonal Anti-E-Cadherin	BD	Ref 610181	1/200
Mouse monoclonal anti-Wt1	Millipore	MAB4234	1/100
Chicken polyclonal anti-GFAP	Millipore	Ref. ab5541	1/200
Mouse monoclonal anti-desmin	Sigma	Ref D1033	1/75
Hamster anti-mucin	Thermo Sci.	HM-1630	1:300
Mouse anti-amylase	Santa Cruz	Sc-46657	1:200
Mouse anti-insulin	Sigma	I2018	1:500

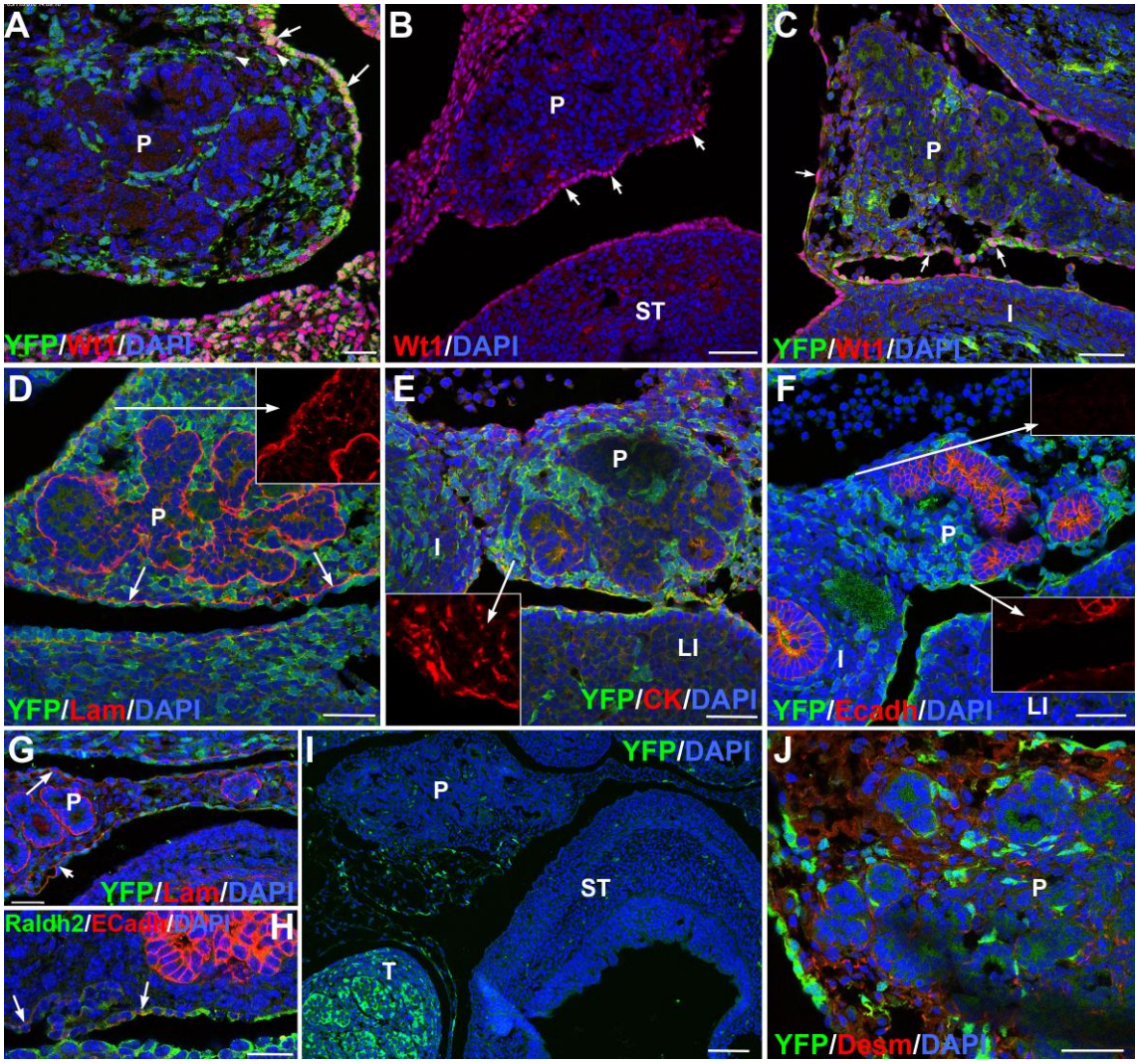
A
P
YFP/Wt1/DAPI
B
P
ST
Wt1/DAPI
C
P
I
YFP/Wt1/DAPI
D
P
YFP/Lam/DAPI
E
P
I
LI
YFP/CK/DAPI
F
P
I
LI
YFP/Ecadh/DAPI
G
P
YFP/Lam/DAPI
H
Raldh2/ECadh/DAPI
I
YFP/DAPI
P
ST
T
J
P
YFP/Desm/DAPI

Figure 1.

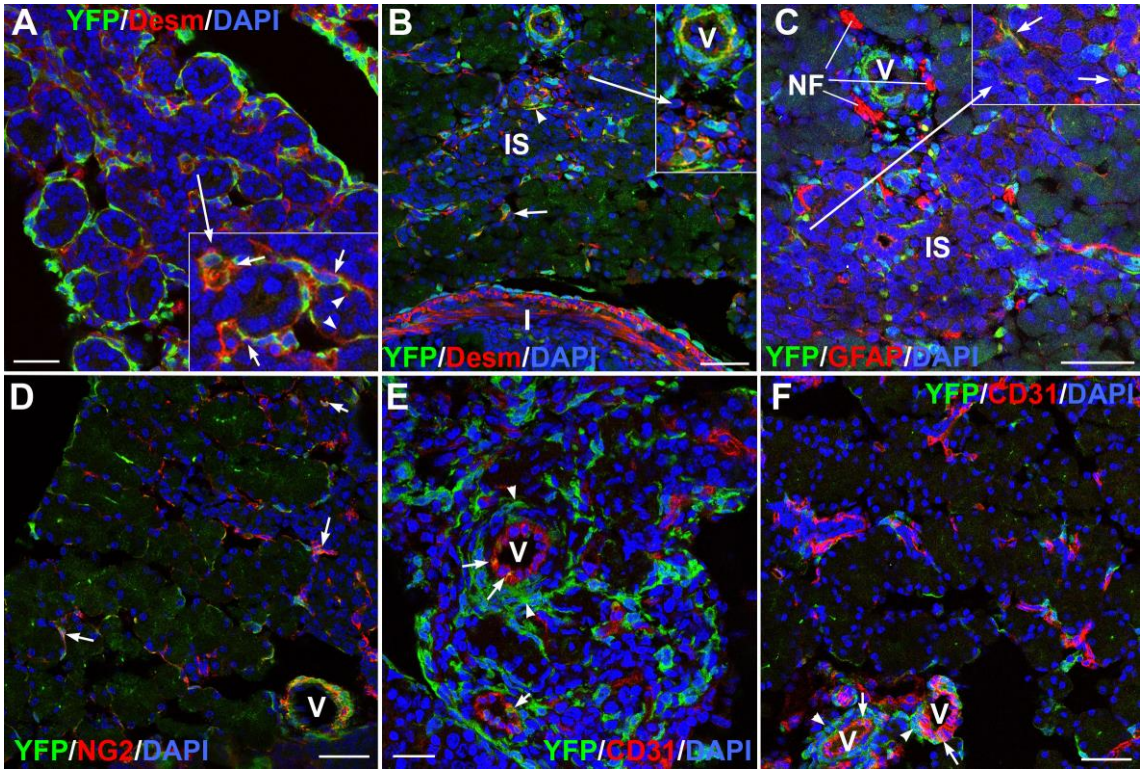

Figure 2

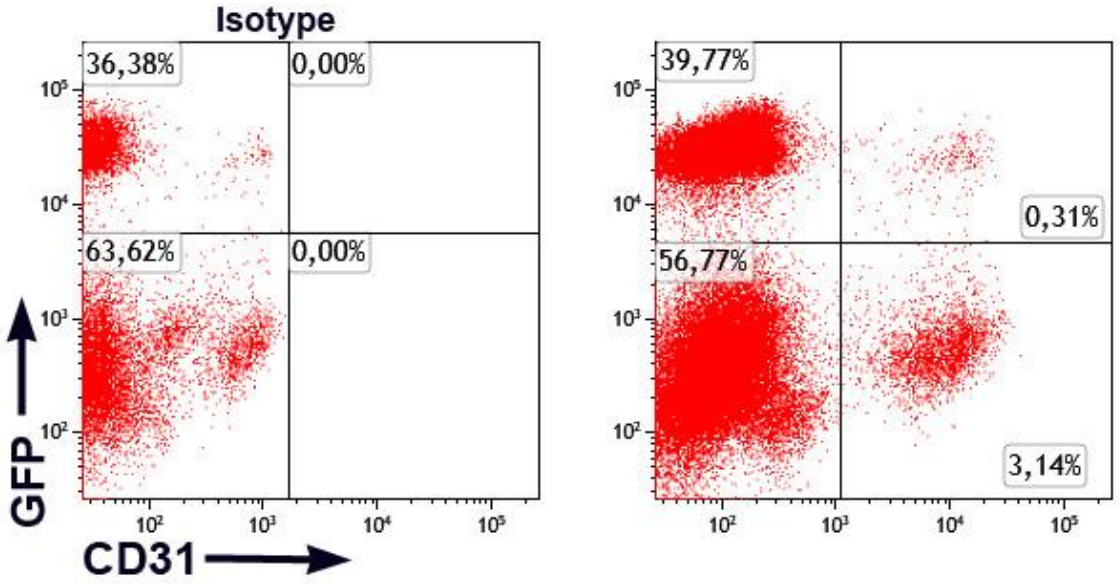

Figure 3

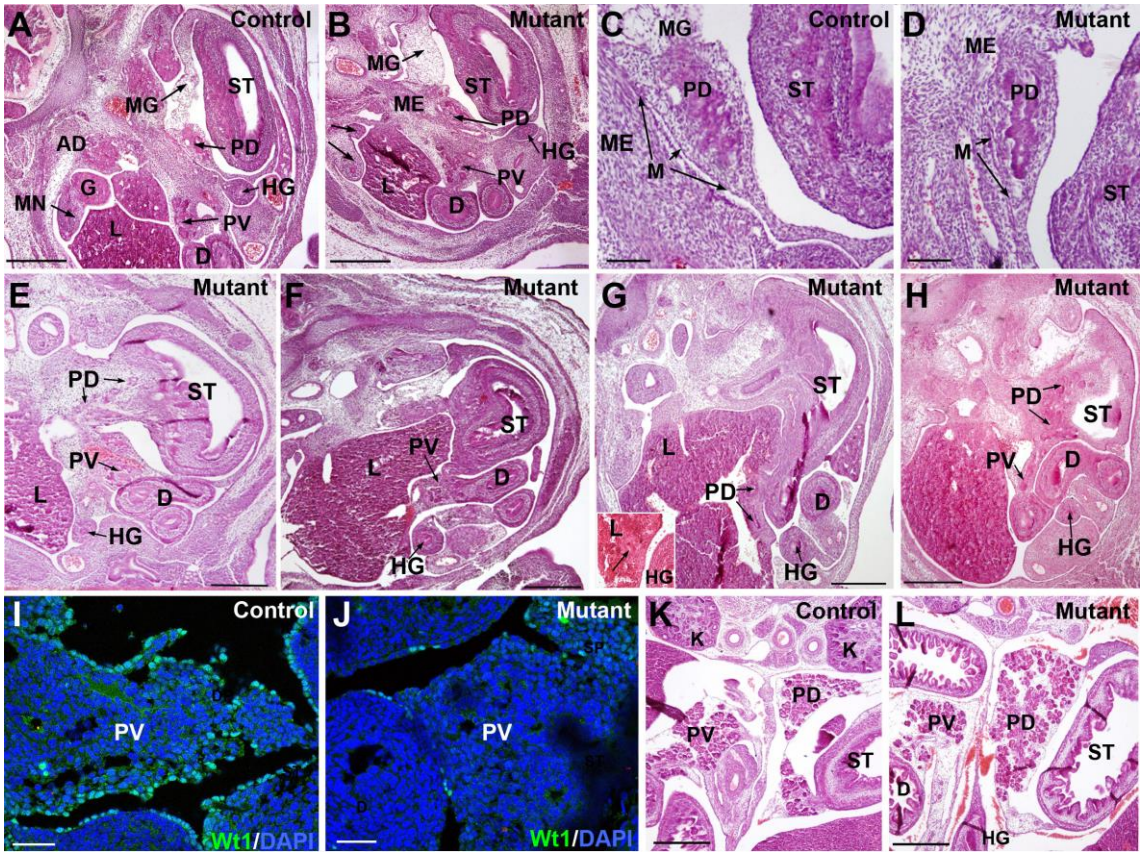

Figure 4

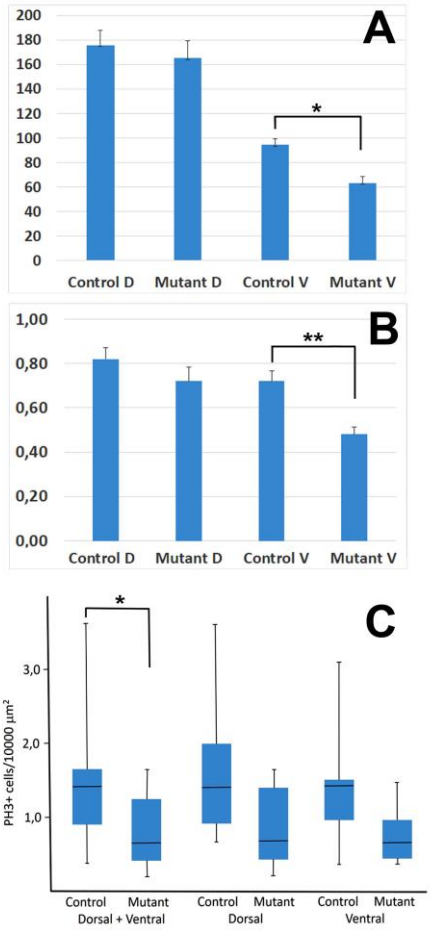

Figure 5

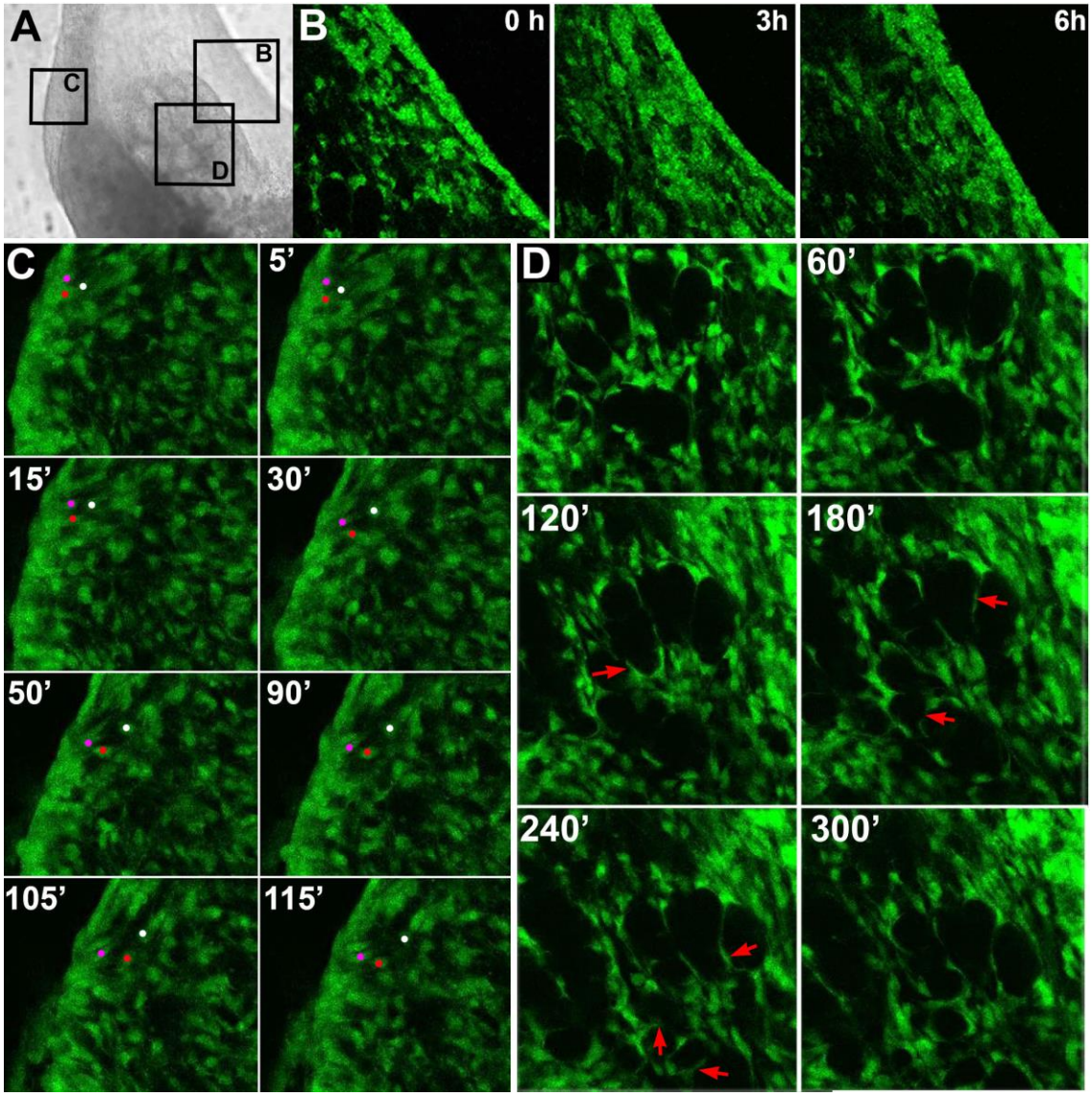

Suppl. Figure 1

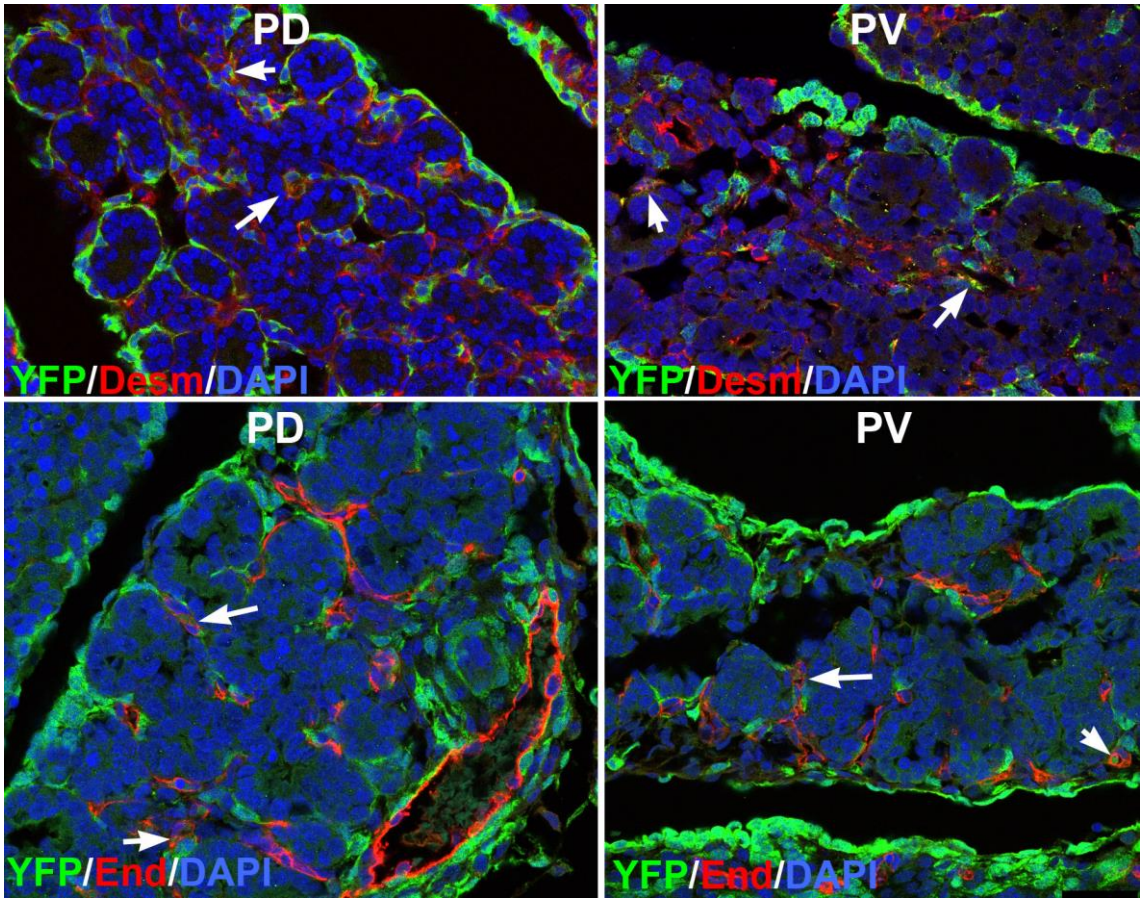

Supplemental figure 2

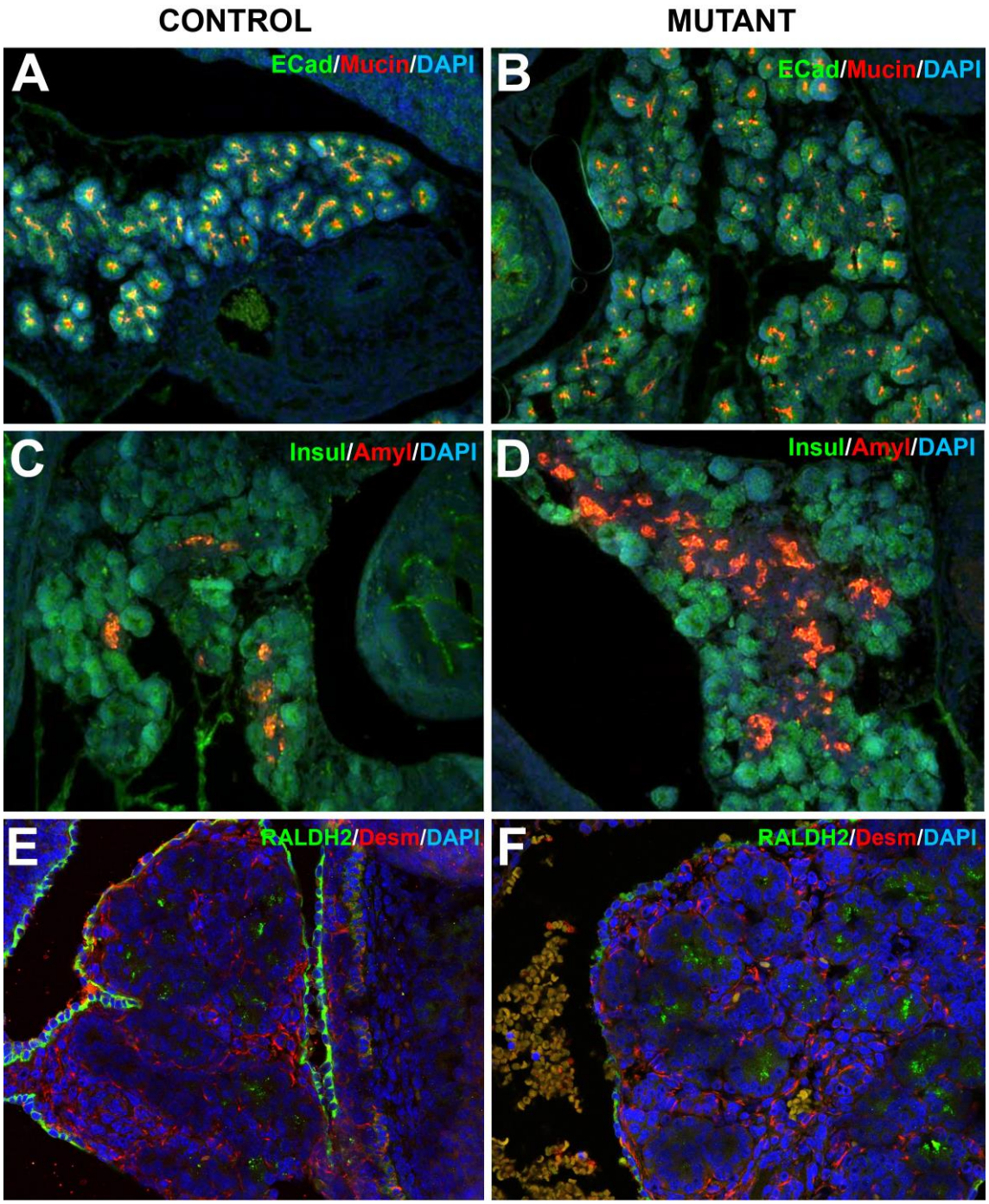

Supplemental figure 3

Supplemental figure 4